CellPress

Molecular Cell
Article

A Pair of RNA-Binding Proteins Controls Networks of Splicing Events Contributing to Specialization of Neural Cell Types

Adam D. Norris,[1] Shangbang Gao,[2] Megan L. Norris,[1] Debashish Ray,[3] Arun K. Ramani,[3] Andrew G. Fraser,[3,4] Quaid Morris,[3,4] Timothy R. Hughes,[3,4] Mei Zhen,[2,4,*] and John A. Calarco[1,*]
[1]FAS Center for Systems Biology, Harvard University, 52 Oxford Street, Cambridge, MA 02138, USA
[2]Lunenfeld-Tanenbaum Research Institute, 600 University Avenue, Toronto, ON M5G 1X5, Canada
[3]Donnelly Centre for Cellular and Biomolecular Research, 160 College Street, Toronto, ON M5S 3E1, Canada
[4]Department of Molecular Genetics, University of Toronto, 1 King's College Circle, Toronto, ON M5S 1A8, Canada
*Correspondence: zhen@lunenfeld.ca (M.Z.), jcalarco@fas.harvard.edu (J.A.C.)
http://dx.doi.org/10.1016/j.molcel.2014.05.004

SUMMARY

Alternative splicing is important for the development and function of the nervous system, but little is known about the differences in alternative splicing between distinct types of neurons. Furthermore, the factors that control cell-type-specific splicing and the physiological roles of these alternative isoforms are unclear. By monitoring alternative splicing at single-cell resolution in *Caenorhabditis elegans*, we demonstrate that splicing patterns in different neurons are often distinct and highly regulated. We identify two conserved RNA-binding proteins, UNC-75/CELF and EXC-7/Hu/ELAV, which regulate overlapping networks of splicing events in GABAergic and cholinergic neurons. We use the UNC-75 exon network to discover regulators of synaptic transmission and to identify unique roles for isoforms of UNC-64/Syntaxin, a protein required for synaptic vesicle fusion. Our results indicate that combinatorial regulation of alternative splicing in distinct neurons provides a mechanism to specialize metazoan nervous systems.

INTRODUCTION

The nervous system has been recognized for over a century as a uniquely complex and diverse organ, composed of various classes of neurons forming precise synaptic connections with partners often located great distances away (Golgi, 1883; Ramón y Cajal, 1890). These anatomical and morphological observations have recently been confirmed and extended by molecular studies identifying genes and proteins that specify and/or discriminate neuronal cell types from each other (Greig et al., 2013; Hobert et al., 2010). However, much is still unknown about the molecular diversity and specification of neuronal cell types and the regulators of such diversity (Hobert et al., 2010).

Alternative pre-messenger RNA (mRNA) splicing, the process by which a single gene encodes multiple isoforms via alternative inclusion or skipping of exons in the mature mRNA, is a pervasive means of regulating gene expression that increases the diversity and complexity of the transcriptome and proteome (Braunschweig et al., 2013; Nilsen and Graveley, 2010). This increased diversity plays an important role in complex organ systems such as the nervous system (Norris and Calarco, 2012; Zheng and Black, 2013), which exhibits high levels of alternative splicing (Barbosa-Morais et al., 2012).

Several studies have identified factors responsible for differential splicing between the nervous system and other tissues (Boutz et al., 2007; Calarco et al., 2009; Gehman et al., 2011; Jensen et al., 2000), but it is not known to what extent differential splicing occurs between different neuronal cell types. While a number of individual cases have been identified (for examples, see Boucard et al., 2005; Chih et al., 2006; Miura et al., 2013), it has remained difficult to study the factors that might control neuron-subtype specificity of alternative splicing. This difficulty is largely due to the technical challenge of accurately measuring splicing differences between cells of the same tissue exhibiting little spatial separation. As such, techniques for visualizing alternative splicing within individual cells of the nervous system or other tissues are highly desirable. The recent use of fluorescent reporters to monitor alternative splicing in cultured cells and in vivo has allowed an exploration of splicing regulation at cellular resolution (Kuroyanagi et al., 2006; Miura et al., 2013; Orengo et al., 2006; Zheng et al., 2013).

Investigations of alternative splicing in the nervous system and other tissues have demonstrated that individual splicing factors regulate networks of exons in sets of functionally related genes (Boutz et al., 2007; Calarco et al., 2009; Ule et al., 2005; Wang et al., 2012; Zhang et al., 2008). Complementary to these genome-wide analyses, focused studies on individual alternative splicing events demonstrate that they are often regulated by multiple splicing factors (Charlet-B et al., 2002; Markovtsov et al., 2000). Although these observations highlight the importance of combinatorial regulation in splicing, nothing is known about how multiple splicing factors act together to shape splicing networks at single neuron resolution.

Characterization of individual target transcripts within splicing networks have identified important splicing events that contribute to specific neuronal phenotypes (Aoto et al., 2013; Raj et al., 2011; Yano et al., 2010). However, the difficulty of

systematic network interrogation in vertebrate models has made it challenging to perform functional analyses of substantial numbers of targets within splicing regulatory networks in vivo. In particular, there is little experimental evidence for how target genes and isoforms within a splicing network contribute to phenotypes associated with loss of a splicing factor.

To address these fundamental challenges in splicing research, we have exploited the nematode *Caenorhabditis elegans*, a well-established model system for studying neurobiology and an increasingly useful model for studying alternative splicing regulation (Barberan-Soler and Zahler, 2008; Barberan-Soler et al., 2011; Ohno et al., 2008; Ramani et al., 2011; Zahler, 2005). We have adapted a two-color splicing reporter to provide a visual survey of alternative splicing events at single-cell resolution in the *C. elegans* nervous system. Remarkably, these reporters reveal that alternative splicing in specific neuronal subtypes occurs frequently and is subject to precise regulation. Characterizing one such alternative splicing event, we performed a genetic screen and identified two highly conserved RNA-binding proteins, UNC-75/CELF and EXC-7/Hu/ELAV, which act together through partially overlapping expression patterns to produce a neuron subtype-specific splicing outcome. We further demonstrate at the genome-wide level that these two factors regulate substantially overlapping target networks of alternative exons. We investigate the exon network of UNC-75 and show that phenotypes observed from the deletion of individual genes in the network are related to phenotypes observed upon loss of the splicing factor. Finally, we demonstrate that this exon network can be used to predict functions for previously uncharacterized genes and isoforms, including two splice variants of the conserved synaptic vesicle fusion protein UNC-64/Syntaxin.

RESULTS

Two Color Reporters Reveal Complex and Diverse Alternative Splicing Patterns within the *C. elegans* Nervous System

To interrogate alternative splicing patterns in vivo at single-neuron resolution in *C. elegans*, we adapted a previously described two-color splicing reporter system (Kuroyanagi et al., 2010; Orengo et al., 2006) (Figure 1A). Alternative exons of interest and their neighboring introns and constitutively spliced exons were cloned upstream of two tandemly positioned open reading frames encoding either enhanced green fluorescent protein (eGFP) or monomeric red fluorescent protein (mRFP). The reporter is engineered so that inclusion or exclusion of the alternative exon leads to switches between the two reading frames. When the alternative exon is skipped, eGFP is read in frame, followed by a stop codon. When the exon is included, the reading frame is shifted so that eGFP is read out of frame and without stop codons, while mRFP is translated in frame. This reporter thus enables monitoring of alternative splicing events in individual cells of live animals by fluorescence microscopy.

We created two-color splicing reporters to monitor the splicing of 14 alternative exons that have been previously confirmed by existing expressed sequence tags/complementary DNA (cDNA) libraries and mRNA sequencing (mRNA-seq) data (Gerstein et al., 2010; Ramani et al., 2011). These exons are highly conserved in several nematode species and are found in genes with known expression and function in the nervous system. It is interesting that, when expressed under the control of a pan-neuronal promoter or endogenous promoters, 7 of 14 of these reporters revealed complex alternative splicing patterns within the nervous system, including differential exon inclusion between different classes of neurons (Figure 1; Table S1 available online).

Monitoring alternative exon 8 in the GTPase *dyn-1*/Dynamin revealed that the exon-included isoform is preferentially expressed in lateral ganglion neurons posterior to the nerve ring, while the exon-excluded isoform predominates in more anteriorly positioned pharyngeal neurons (Figure 1C). The serotonin-gated chloride channel *mod-1* revealed another unique pattern of differential exon usage in specific head neurons (Figure 1E). The neuronal serine/threonine protein kinase gene *sad-1* encodes two isoforms that are coexpressed in most neurons in the head and ventral nerve cord, but only one isoform is expressed in a cluster of oxygen-sensing cells, while only the other isoform is expressed in a nearby cluster of lateral mechanosensory neurons (Figure 1D). A striking differential splicing pattern was observed with a reporter monitoring alternative exon 16 of *unc-16*/JIP3 in the ventral nerve cord, which is composed of excitatory cholinergic and inhibitory GABAergic motor neurons. The exon-16-included isoform is expressed in both cholinergic and GABAergic neurons (Figures 1F and 1G), while the excluded isoform is expressed only in GABAergic neurons, confirmed by coexpressing a codon-optimized enhanced blue fluorescent protein (eBFP) in GABAergic neurons (Figure 1F).

All reporters with neuron-specific splicing displayed a unique regulatory pattern. Notably, the patterns observed in each individual reporter were identical from animal to animal, indicating that splicing was being actively regulated and was not the result of purely stochastic processes. Taken together, these results demonstrate that alternative splicing patterns in *C. elegans* are frequently differentially regulated in specific neurons.

A Pair of RNA-Binding Proteins, UNC-75 and EXC-7, Control Differential Splicing in Ventral Cord Motor Neurons

To identify factors regulating motor neuron-specific alternative splicing, we conducted a microscopy-based genetic screen (Figure 2A) using the *unc-16* exon 16 reporter described earlier. Worms carrying this reporter were subjected to ethyl methanesulfonate (EMS) mutagenesis, and their F_2 progeny were visually screened for disruptions in the GABAergic motor neuron-specific splicing pattern.

From ~7,000 haploid genomes screened, we recovered two viable mutants belonging to distinct complementation groups and identified the causal mutations in these animals by whole-genome sequencing (Bigelow et al., 2009). These mutations were found in two genes encoding RNA-binding proteins: *unc-75*, a member of the CELF family, and *exc-7*, a member of the Hu/ELAV family (Figure 2B). Both RNA-binding proteins are conserved from *C. elegans* to humans (Loria et al., 2003), where they are expressed in neurons, and are implicated in a number of neurological conditions (Dasgupta and Ladd, 2012). In *C. elegans* and mammals, these factors have been shown to

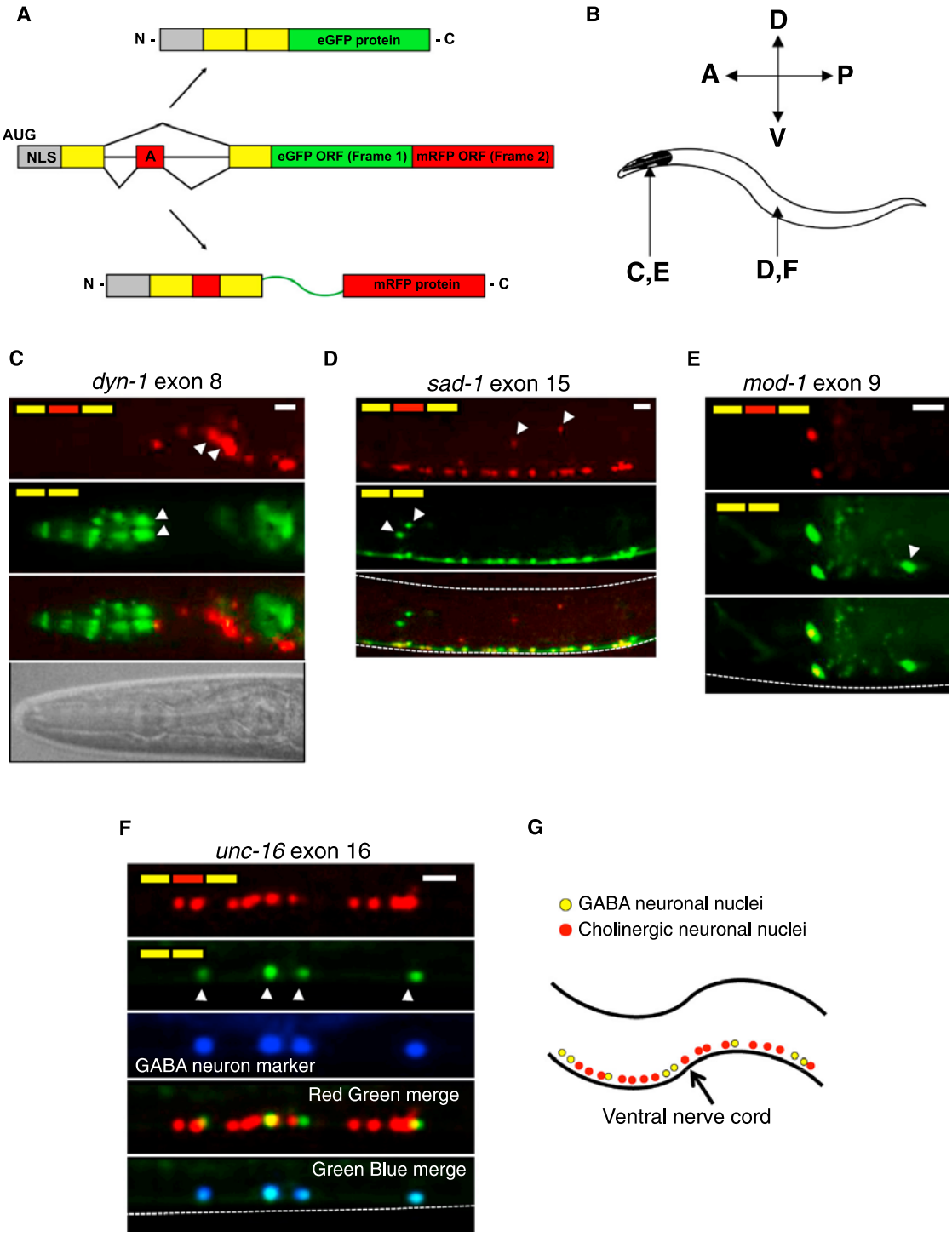

Figure 1. Two-Color Splicing Reporters Reveal Diversity of Alternative Splicing within the Nervous System

(A) Schematic of two-color splicing reporter. An alternative exon (red box with letter A) and its neighboring intron and exon sequences (yellow boxes) are cloned upstream of EGFP and mRFP open reading frames (ORFs; larger red and green boxes). Skipping of the alternative exon leads to translation of EGFP, while inclusion of the exon leads to translation of mRFP. An SV40 nuclear localization signal (NLS; gray box) is included in the reporter to focus the signal in the nucleus. (B) Anatomical reference for (C)–(F), indicating the location: head for (C) and (E) or midbody area for (D) and (F). D, dorsal; V, ventral; A, anterior; P, posterior. (C–F) Fluorescence images of two-color splicing reporters for neuronal alternative splicing events. White arrowheads indicate select nuclei with unique isoform usage patterns. All animals are at larval stage L4. Dashed lines delineate borders of the worms. In (C), a brightfield image is included to serve as a reference,

(legend continued on next page)

regulate several steps of RNA metabolism, including the regulation of splicing (Barberan-Soler et al., 2011; Darnell, 2013; Dasgupta and Ladd, 2012; Kuroyanagi et al., 2013a).

The molecular lesion in our *unc-75*(*csb7*) mutant introduces a premature termination codon in the linker region of the protein, and the lesion in our *exc-7(csb6)* mutant creates a Gly-to-Arg substitution in a conserved amino acid of the second RNA recognition motif (Figure 2B). While the *unc-75(csb7)* allele we recovered in our screen behaved similarly to the reference *unc-75(e950)* null allele (Loria et al., 2003), our *exc-7(csb6)* allele exhibited more modest effects on alternative splicing in RT-PCR assays relative to the *exc-7(rh252)* null allele (Fujita et al., 2003; Figure 2D and Figure S2). These data suggest that our *csb6* allele may be a hypomorphic allele. We therefore carried out all further experiments using the reference null alleles of *unc-75* and *exc-7*.

In both *unc-75* and *exc-7* mutants, the skipped isoform loses its restricted expression, becoming aberrantly expressed in cholinergic ventral nerve cord motor neurons (Figure 2C), and indicating that UNC-75 and EXC-7 both mediate inclusion of exon 16. In *unc-75; exc-7* double mutant animals, exon inclusion is lost entirely (Figure 2C). Transgenic expression of wild-type UNC-75 or EXC-7 in the respective *unc-75* or *exc-7* mutants rescued *unc-16* splicing defects (Figure S1). We performed RT-PCR assays with primers specific to the splicing reporter mRNA (Figure 2D, upper panel) or endogenous *unc-16* mRNA (Figure 2D, lower panel) and confirmed that our reporter recapitulates the endogenous regulation of this alternative exon. The difference in overall ratios of included to skipped isoforms between the splicing reporter and endogenous mRNA is likely due to *unc-16* also being expressed in nonneuronal tissues, where the skipped isoform predominates (Kuroyanagi et al., 2013b), while our splicing reporter was driven by a panneuronal promoter.

Previous reports, which we have confirmed (data not shown), indicated that UNC-75 is expressed panneuronally (Loria et al., 2003), while EXC-7 is expressed in cholinergic but not in GABAergic motor neurons (Fujita et al., 1999), suggesting that their partially overlapping expression patterns could explain the differential splicing of *unc-16* exon 16. If GABAergic motor neurons express only UNC-75, exon inclusion should still be observed in these neurons in *exc-7* mutant animals but not in *unc-75* mutants. Indeed, in an *unc-75* mutant, GABAergic motor neurons expressed only the skipped isoform, whereas in an *exc-7* mutant, both the included and the skipped isoforms were expressed in GABAergic neurons (Figure S2). These results indicate that, in GABAergic motor neurons, UNC-75 partially stimulates exon 16 inclusion, whereas in cholinergic motor neurons, UNC-75 and EXC-7 together promote complete inclusion of exon 16.

UNC-75 and EXC-7 Directly Control *unc-16* Alternative Splicing by Binding to Sequences in the Downstream Intron

To determine if UNC-75 and EXC-7 directly control *unc-16* exon 16 alternative splicing by binding to its pre-mRNA, we identified consensus motifs bound in vitro by recombinant UNC-75 and EXC-7 proteins using RNAcompete (Ray et al., 2013). The UNC-75 and EXC-7 consensus sequences identified were U[G/A]UUGUG and UAAGUU, respectively (Ray et al., 2013) (Figure 3A), which are in close agreement with motifs recognized by their vertebrate homologs (Ray et al., 2013). Our UNC-75 consensus motif also agrees with a recently described UNC-75-targeted U/G-rich sequence (Kuroyanagi et al., 2013b). We conducted electrophoretic mobility shift assays (EMSAs) by incubating recombinant glutathione-S-transferase-tagged UNC-75 and EXC-7 proteins with RNA oligonucleotides containing consensus motifs or sequences with nucleotide substitutions at highly constrained positions in each motif. Both factors bound RNAs containing consensus binding motifs but displayed reduced binding to RNAs with substitutions in the motifs (Figure S3).

The *unc-16* pre-mRNA contains an EXC-7 consensus binding sequence in the intron downstream of alternative exon 16, as well as two UNC-75 consensus sequences—one in exon 16 and one in the downstream intron (Figure 3B). To test whether these sites are functional *cis*-elements controlling exon 16 alternative splicing in vivo, we created two-color splicing reporters containing substitutions in the consensus binding motifs tested in our EMSAs (Figure S3). While mutating the exonic UNC-75 consensus binding motif did not affect alternative splicing, mutating either the UNC-75 or EXC-7 intronic consensus binding motifs caused an increase in exon skipping (Figure 3C), consistent with what was observed in our *unc-75* and *exc-7* mutants (Figure 2C). When all three consensus motifs were mutated, exon inclusion was nearly undetectable, consistent with the phenotype of the *unc-75; exc-7* double mutant (Figures 2C and 3C). These results strongly support a model in which UNC-75 and EXC-7 combinatorially control neuron subtype-specific splicing of *unc-16* exon 16 by directly binding the pre-mRNA in the downstream intron and mediating exon inclusion (Figure 3D).

UNC-75 and EXC-7 Regulate Extensive and Overlapping Exon Networks

To assess whether UNC-75 and EXC-7 more generally regulate alternative splicing in a combinatorial manner, we performed high-throughput transcriptome sequencing (mRNA-seq) analyses of wild-type, *unc-75*, *exc-7*, and *unc-75; exc-7* mutant whole animals. We searched for transcripts displaying statistically significant differences of > 20% in relative exon junction usage between wild-type animals and each of the mutant strains (Figures 4A and 4B). Using these criteria, we tested 48 junction difference predictions by semiquantitative RT-PCR, and 46/48 (96%) were validated (Figure 4B and Figure S4A; data not shown).

We identified hundreds of differentially utilized exon junctions that varied between wild-type and one of the three mutant strains by >20% (Figures 4A and 4B; Table S2). The

highlighting that the green anterior cells (white arrowheads) are likely pharyngeal neurons. In (F), GABAergic motor neurons are labeled with *Punc-25*::BFP. Scale bar, 10 μm.

(G) Simplified model of the organization of GABAergic (yellow) and cholinergic (red) motor neurons in the ventral nerve cord.

See also Table S1.

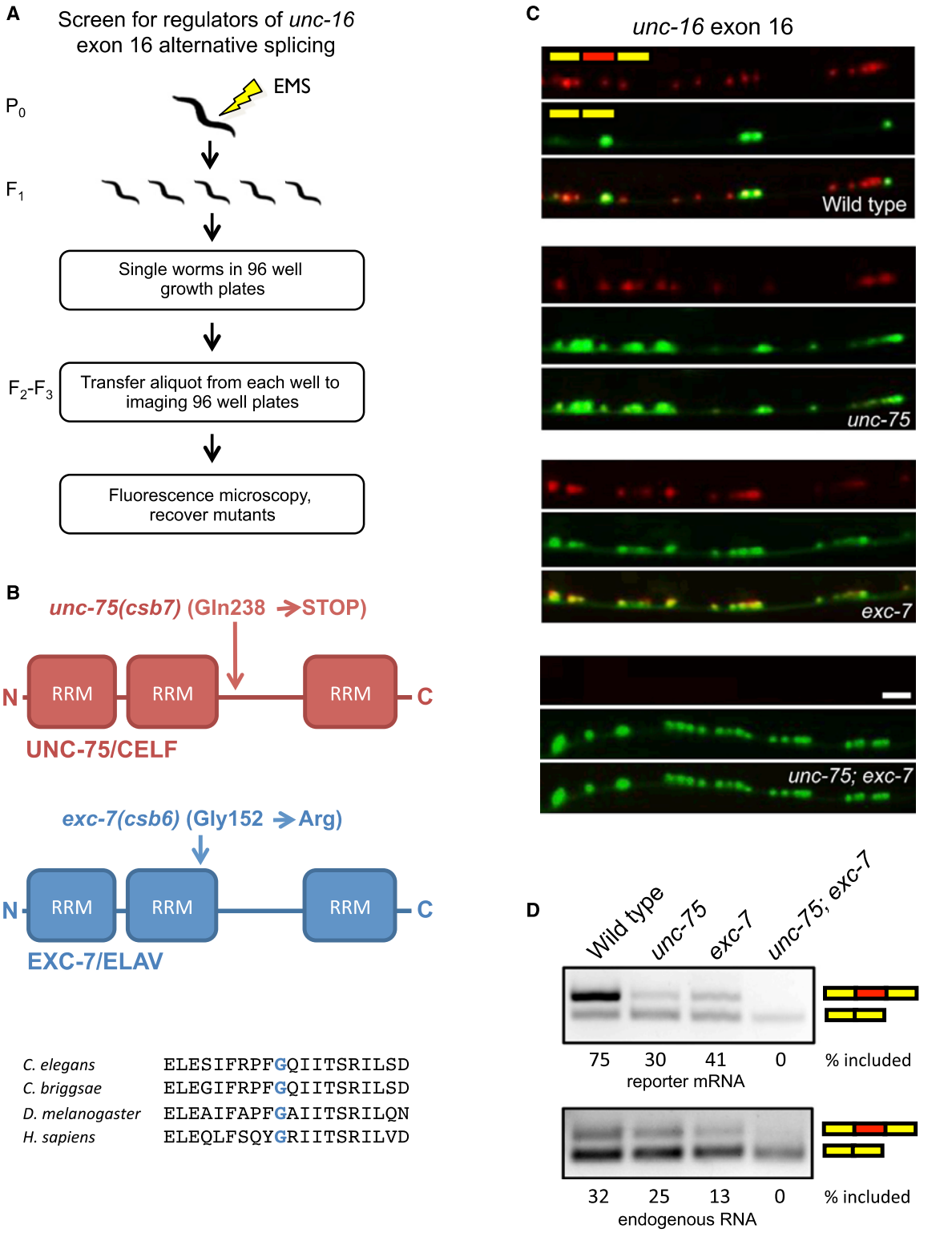

Figure 2. Genetic Screen for Regulators of *unc-16* Alternative Splicing Identifies Two RNA-Binding Proteins that Act Combinatorially

(A) Schematic of microscopy-based EMS mutagenesis screen.

(B) Domain structure of screen hits and molecular nature of genetic lesions.

(C) *unc-16* alternative splicing phenotypes in *unc-75* and *exc-7* mutants. Scale bar, 10 μm.

(D) RT-PCR analysis of *unc-16* two-color reporter mRNA (upper panel) or endogenous *unc-16* mRNA (lower panel).

See also Figures S1 and S2.

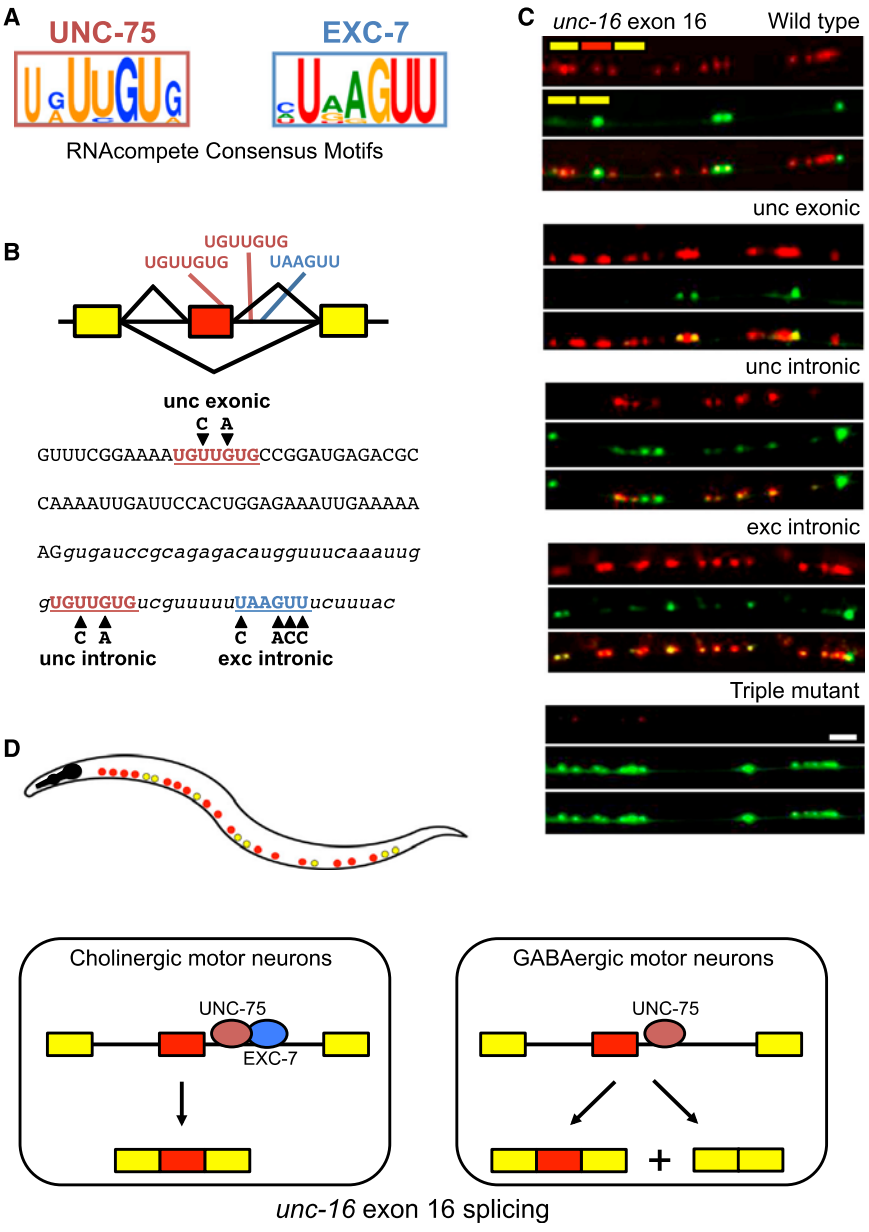

Figure 3. UNC-75 and EXC-7 Regulate *unc-16* Exon 16 Splicing by Binding to Consensus Motifs in Its Downstream Intron

(A) Consensus binding motifs as determined by RNAcompete.

(B) Presence of consensus binding motifs in *unc-16* exon 16 and its downstream intron. Mutations introduced into the motifs are indicated in bold black letters.

(C) Two-color splicing reporters for *unc-16* exon 16 were created with the mutations shown in (B) and expressed in wild-type worms. Scale bar, 10 μm.

(D) Model for regulation of exon 16 alternative splicing. In cholinergic motor neurons (red dots in worm diagram), both UNC-75 and EXC-7 bind to *cis* elements in the intron downstream of *unc-16* alternative exon 16, promoting full exon inclusion. In GABAergic motor neurons (yellow dots in worm diagram), only UNC-75 is present and its binding to the pre-mRNA promotes partial exon inclusion.

See also Figure S3.

most abundant classes of differential junction usage involved alternative inclusion of exons, alternative first exons, and alternative 5′ splice sites, with each class representing about one quarter of the total exon junction differences observed (Figure S4B). Among exon inclusion events that are differentially spliced between wild-type and *unc-75; exc-7* double mutants, 51 exons exhibit increased skipping in the double mutant, versus only 19 with increased inclusion, suggesting that UNC-75 and EXC-7 primarily mediate inclusion of exons.

Our genome-wide analysis revealed distinct modes of individual and combinatorial control of alternative junction usage by UNC-75 and/or EXC-7, and we confirmed these examples by RT-PCR analysis and two-color splicing reporters (Figure 4B; Figures S4A and S4C). A substantial cluster of junctions was regulated by UNC-75 and EXC-7 (Figure 4B, "Coregulated"). In these cases, *unc-75* and *exc-7* mutants alone have similar but modest effects on junction usage, while the double mutant has more robust changes, displaying either additive or synergistic effects on splicing regulation. The *unc-16* exon 16 alternative splicing regulatory pattern belongs to this "Coregulated" category. We also identified a smaller set of junctions that were combinatorially regulated, but in these cases, each single mutant displayed an opposite regulatory outcome relative to wild-type and the double mutant had an intermediate effect (Figure 4B, "Antagonistic"). Altogether, we found that 31% of the spliced junctions regulated by *unc-75* are also regulated by *exc-7* (Figures 4A and 4B), demonstrating overlap between UNC-75 and EXC-7 targets. Additionally, 53% of all differentially regulated junctions between wild-type and *unc-75; exc-7* double mutants were not found to be differentially regulated in either of the single mutants (Figures 4A and 4B). These results demonstrate extensive regulatory cooperativity between these two RNA-binding proteins.

To extend our mechanistic studies of *unc-16* exon 16 alternative splicing described earlier, we searched full exon or intron sequences surrounding the 51 exons with increased skipping in *unc-75; exc-7* double mutant animals for the presence of UNC-75 or EXC-7 binding sites identified by RNAcompete. Compared to a control set of similarly matched exons or introns that are not regulated by either RNA-binding protein, we found a significant enrichment of both *unc-75* and *exc-7* binding sites in the downstream intron following the cassette exon

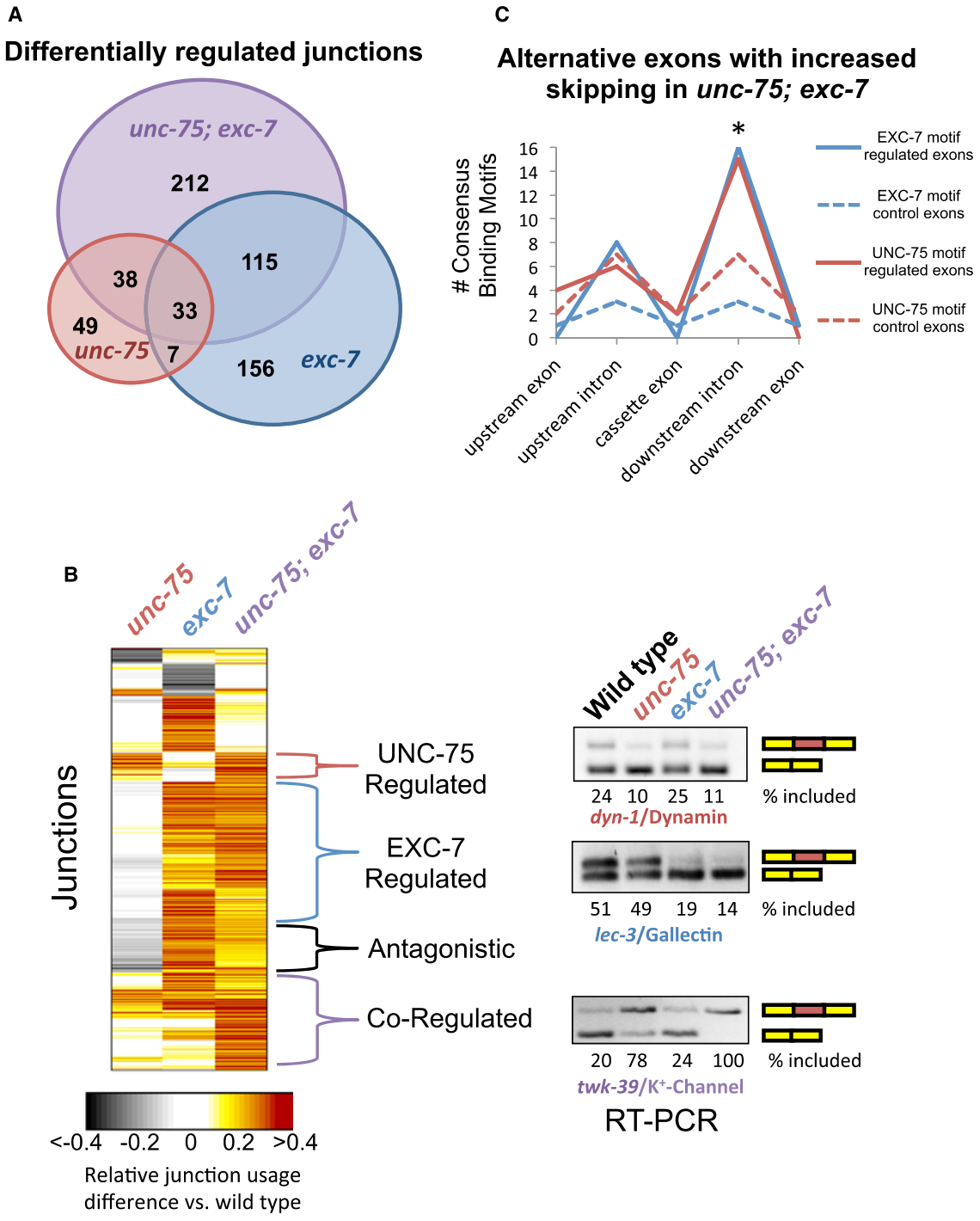

Figure 4. UNC-75 and EXC-7 Regulate Partially Overlapping Sets of Alternative Junctions

(A) Venn diagram displaying number of statistically significant alternative junction changes between wild-type and any of the three mutant conditions, as well as the overlap among the three conditions.

(B) Heat map displaying differential junction usage (rows) between wild-type and mutant conditions (columns). All junction difference values were normalized to the double mutant comparison. Right panel shows representative RT-PCR validations of alternative splicing events belonging to different regulatory modes.

(C) Presence of *exc-7* or *unc-75* binding motifs in the vicinity of 51 cassette exons that undergo increased skipping in *unc-75; exc-7* double mutants.

See also Figures S4 and S5 and Table S2.

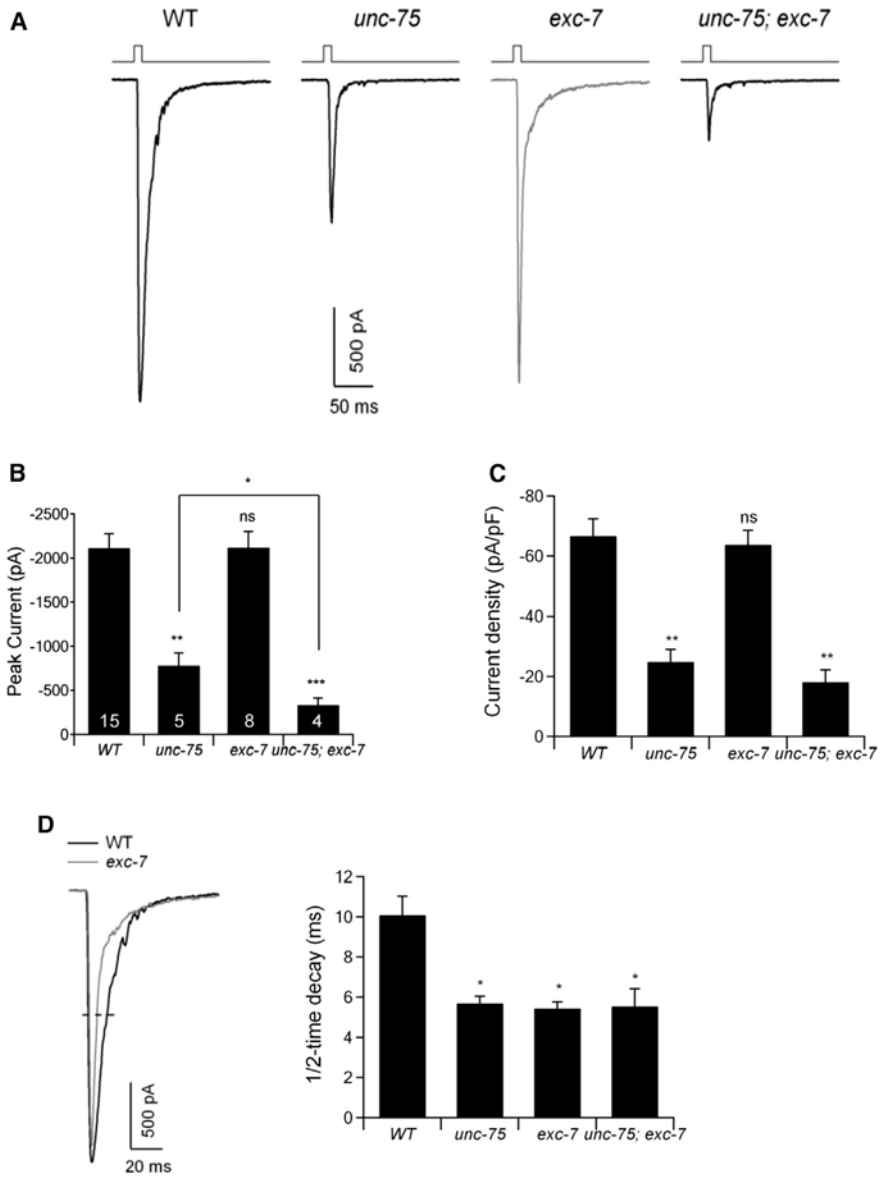

Figure 5. *unc-75* and *exc-7* Mutants Exhibit Partially Overlapping Cholinergic Synaptic Transmission Defects at the Neuromuscular Junction

(A) Representative traces of evoked EPSCs in wild-type (WT), *unc-75(e950)*, *exc-7(rh252)*, and *unc-75(e950); exc-7(rh252)* mutants. Muscles were holding at −60 mV. The EPSCs were induced by 10 ms blue light (top traces) in a *zxIs6* background, expressing Channelrhodopsin-2 in cholinergic neurons.

(B and C) The amplitude (B) and density (C) of currents in wild-type and mutant strains. Data are represented as mean ± SEM.

(D) The half-time decay of the EPSCs in wild-type and mutant animals. *p < 0.05; **p < 0.01; ***p < 0.001; ns, not significant by Mann-Whitney U test. Numbers in the bar graph indicate the number of animals examined for each genotype.

See also Figure S6.

(Figure 4C, p < 0.05, chi-square test). Performing the same analysis on the 19 exons with increased inclusion in the double mutant yielded no enrichment of such binding-site patterns (Figure S5). These results are consistent with our experiments with the *unc-16* exon16 alternative splicing reporter (Figures 3C and 3D), and they also agree with recent data reported (Kuroyanagi et al., 2013b), suggesting that UNC-75 generally stimulates exon inclusion by binding to downstream intronic sequences.

Gene ontology analysis revealed that genes regulated only by UNC-75 are enriched in functions related to ion channels and transporters, while those regulated only by EXC-7 are enriched in functions related to behavior and gamete generation (Table S3). Taken together, our genome-wide analysis indicates that UNC-75 and EXC-7 control isoform usage in partially distinct but overlapping networks of transcripts with neuronal functions.

UNC-75 and EXC-7 Control Cholinergic Synaptic Transmission through Partially Distinct Mechanisms

Previous work has demonstrated that both *unc-75* and *exc-7* mutants are resistant to the acetylcholinesterase inhibitor aldicarb, implying that these mutants exhibit reduced cholinergic synaptic transmission (Loria et al., 2003). Moreover, an *unc-75; exc-7* double mutant exhibits a more severe aldicarb resistance phenotype than either of the single mutants, implying that *unc-75* and *exc-7* have nonredundant functional roles (Loria et al., 2003).

To more directly test if these mutants exhibit combinatorial synaptic transmission defects, we generated *unc-75*, *exc-7*, and double mutant animals expressing Channelrhodopsin-2, a light-gated ion channel that enables precise activation of neurotransmission by pulses of light (Liewald et al., 2008). We expressed Channelrhodopsin-2 in cholinergic motor neurons and recorded spontaneous miniature postsynaptic currents (mPSCs) and evoked excitatory postsynaptic currents (EPSCs) across the neuromuscular junction in body wall muscles on light-stimulated cholinergic motor neuron activation (Gao and Zhen, 2011; Goodman et al., 2012). Stimulation of cholinergic motor neurons in wild-type animals elicited a robust EPSC (Figures 5A and 5B). In *unc-75* mutants, this evoked response was significantly diminished, whereas *exc-7* mutants exhibited no change in the amplitude or density of the evoked current (Figures 5A–5C). However, *unc-75; exc-7* double mutants exhibited significantly lower evoked amplitude than *unc-75* single mutants did (Figures 5A and 5B). We also observed that the half-time decay of the evoked response is similarly shorter in *exc-7*, *unc-75*, and double mutants relative

to wild-type animals (Figures 5A and 5D). The frequency, but not the amplitude, of mPSCs was significantly reduced in each of the single mutants and the double mutants (Figure S6). These results indicate that, while both UNC-75 and EXC-7 affect cholinergic synaptic transmission, UNC-75 plays a more critical role, although UNC-75 can only partially compensate for the loss of EXC-7.

Analysis of the UNC-75 Exon Network Reveals Neuronal Phenotypes for Known and Uncharacterized Genes

unc-75 mutants exhibit severe neuronal phenotypes, including uncoordination and altered aldicarb sensitivity. Given that UNC-75 also controls a network of exons in genes enriched for neuronal functions, we reasoned that analysis of this network might reveal phenotypic relationships among loss-of-function mutations in UNC-75 target genes. It is striking that, among 118 genes identified by our genome-wide analysis regulated by UNC-75, >25% have been reported to exhibit loss-of-function uncoordinated and/or altered aldicarb sensitivity phenotypes (Figures 6A and 6B). This percentage is likely an underestimate of the true proportion of UNC-75-regulated genes with such phenotypes, given that most genes studied in previous reports were not assessed for changes in aldicarb sensitivity or for more subtle quantifiable effects on locomotion (Figures 6A and 6B).

These results suggested that the UNC-75 exon network can be used to predict functions for genes with previously uncharacterized phenotypes. Therefore, we tested available mutant strains harboring loss of function alleles corresponding to 12 conserved genes with UNC-75-regulated exons for locomotion or aldicarb sensitivity defects. It is interesting that the majority (67%) of these alleles exhibited one or both phenotypes (Figures 6A and 6C; Figures S7A and S7B). Several of the genes in our analysis have no known molecular function, while some have been studied in other tissues or in other organisms, which could shed light on their role in neurobiology. For example, we determined that animals carrying mutations in the gene *acs-13*, encoding an acyl coenzyme A (CoA) synthetase enzyme implicated in fatty acid metabolism, exhibit altered aldicarb sensitivity.

Taken together, our results indicate that interrogation of exon networks can be used as an alternative and effective approach to identify regulators of synaptic transmission and behavior. For instance, a previous aldicarb resistance RNA-interference-based screen against genes predicted to be involved in synaptic localization, cytoskeletal regulation, or membrane trafficking had a positive hit rate of 8.9% (Sieburth et al., 2005), compared with our 47% positive hit rate for the aldicarb phenotype in the UNC-75 alternative splicing network analysis (Figure 6C).

Isoform-Specific Functions for a Central Gene in the UNC-75 Regulatory Network

In addition to using the exon network to predict gene function, we further tested whether UNC-75-regulated isoforms have distinct neuronal functions in vivo. We focused on the A and B isoforms of the gene *unc-64/Syntaxin*, a critical component of the SNARE complex that mediates vesicle and membrane fusion (Ogawa et al., 1998; Saifee et al., 1998). The relative usage of its mutually exclusive final exons A and B is combinatorially regulated by UNC-75 and EXC-7 (Figure 6D), and these exons encode slightly different transmembrane domains for insertion into the presynaptic membrane. *unc-64* mutants, like *unc-75* mutants, are uncoordinated and resistant to aldicarb (Saifee et al., 1998). We utilized fosmid recombineering (Tursun et al., 2009) to create transgenes that selectively express a single isoform and assessed the rescuing capacity of each isoform in *unc-64* loss-of-function mutant animals. Both isoforms equivalently rescued the aldicarb resistance phenotype of mutant animals, suggesting that each isoform was functional (Figure 6E). It is intriguing, however, that only the B isoform efficiently rescued the uncoordination phenotype (Figure 6E; Movie S1). These results indicate that *unc-64* isoforms A and B have nonoverlapping functions and that the relative proportions of these isoforms are fine-tuned by UNC-75. Our data also suggest that the UNC-75 regulatory network can be used to uncover nonredundant roles for isoforms in the nervous system.

DISCUSSION

Neuron-Specific Alternative Splicing Occurs Frequently and Is Subject to Precise Regulation

While cases of alternative splicing between cells in the nervous system have previously been identified by serendipity, studies have been limited by the technical challenges of observing splicing differences in individual neurons. In this study, we have developed a framework to better understand differential splicing regulation at single-neuron resolution. Using *C. elegans* as a model system, we found that a striking 50% of alternative exons tested with our two-color reporters exhibit neuron-specific alternative splicing patterns (Figure 1). These patterns include differences between distinct functional classes of neurons. The deterministic regulation of alternative splicing in single neurons described here contrasts with recent observations of neuron-specific stochastic regulation of exon choice in *Drosophila dscam1* gene transcripts (Miura et al., 2013). These observations suggest that both deterministic and stochastic variation in splicing generate cellular and molecular diversity in the nervous system. Our results highlight the importance of investigating gene regulation and alternative splicing at the level of individual cells and complement recent transcriptome-wide analyses of splicing conducted at single-cell resolution (Shalek et al., 2013).

Analysis of Exon Networks Identifies Genes with Important Neuronal Functions

Previous studies have led to the hypothesis that splicing factor-mediated control of networks of transcripts might serve to specialize the function of specific tissues (Calarco et al., 2009; Ule et al., 2005; Wang et al., 2012; Zhang et al., 2008). Our results support and extend this paradigm at the level of individual neuronal cells. The shared phenotype between the loss of many single UNC-75 targets and loss of UNC-75 itself makes it tantalizing to hypothesize that the *unc-75* phenotype may be directly caused by cumulative effects of misregulated splicing of target genes in the alternative splicing network (Figure 7A).

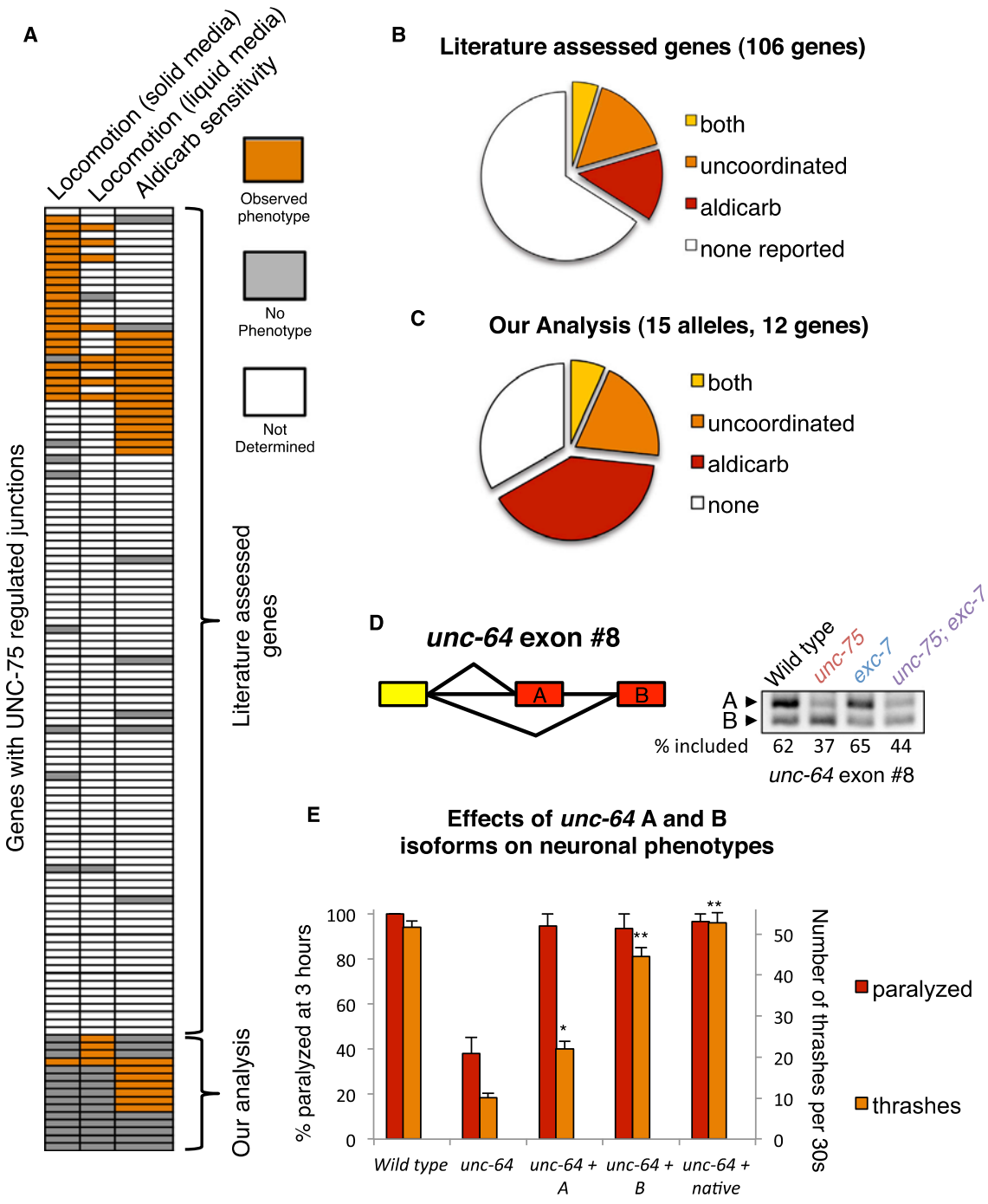

Figure 6. Network Analysis of *unc-75*-Regulated Transcripts Reveals a Coherent Network and Predicts Neuronal Phenotypes

(A) Heat map displaying presence or absence of uncoordination (first and second columns) or aldicarb-sensitivity phenotypes (third column) in the UNC-75 network of genes based on previously reported phenotypes from the literature and our analysis of genes with previously uncharacterized phenotypes. Uncoordination phenotypes were separated on the basis of whether a phenotype could be observed on solid media (first column) or quantitatively through thrashing assays in liquid media (second column).

(B and C) Proportion of target genes exhibiting one or both phenotypes in the literature search (B) or our knockout allele analysis (C).

(D) Left: schematic showing alternative splicing at the 3′ end of *unc-64* gene transcripts. Right: RT-PCR assay showing differential splicing patterns in *unc-75*, *exc-7*, and double mutants relative to wild-type animals.

(E) Fosmid-based isoform-specific reintroduction of UNC-64/Syntaxin isoforms into an *unc-64* loss-of-function background reveals isoform-specific differences among the two splice variants. Data represented as mean ± SEM.

See also Figure S7, Table S3, and Movie S1.

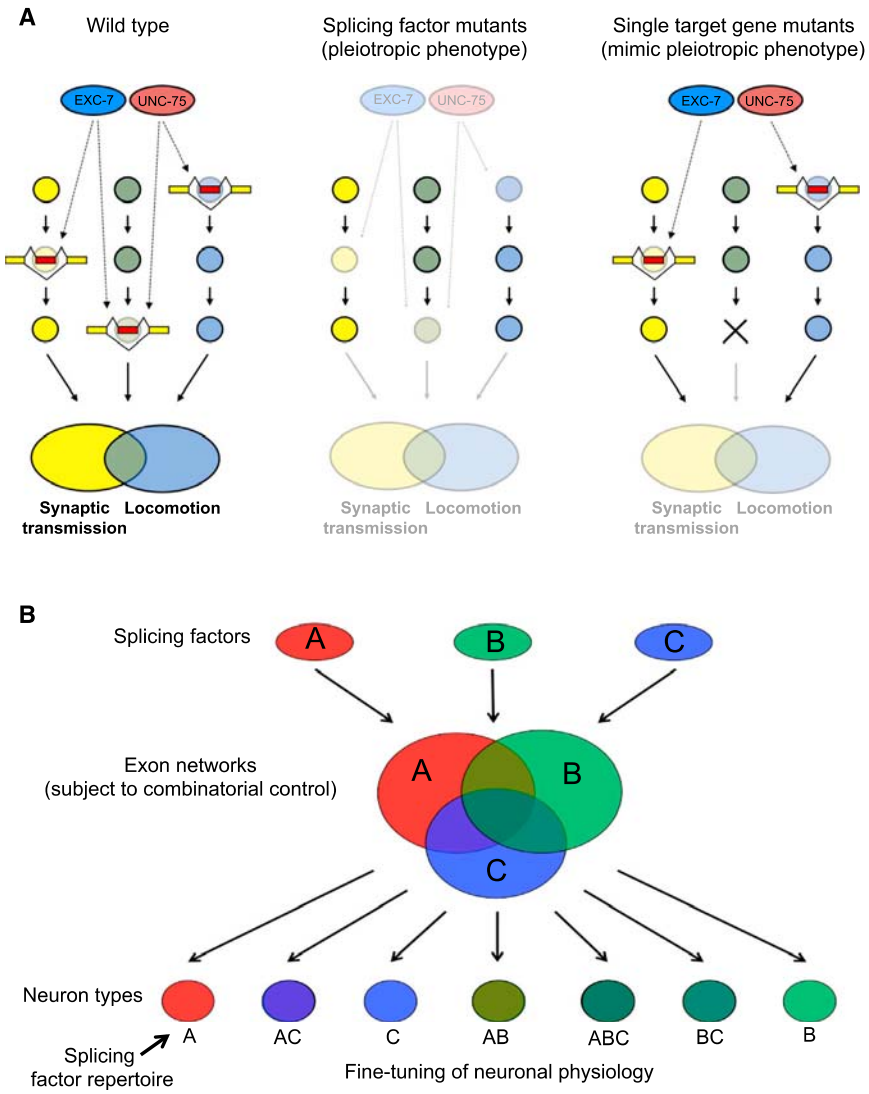

Figure 7. Models for the Contribution of UNC-75 and EXC-7 Splicing Networks to Neuronal Physiology

(A) In wild-type animals (left panel), UNC-75 and EXC-7 (red and blue ovals, respectively) regulate partially distinct sets of splicing events (yellow and red boxes) in target genes (yellow, light blue, and light green circles) found in pathways controlling synaptic transmission and locomotion. When these factors are absent (middle panel), cumulative effects of misregulated splicing of these target gene transcripts can lead to observable locomotion and/or synaptic transmission phenotypes. However, complete loss of function of individual splicing network target genes found in critical pathways (right panel, marked by an X) are often sufficient to produce phenotypes found in the splicing factor mutants.

(B) The action of three splicing factors (red, blue, and green ovals) with overlapping expression patterns regulate overlapping exon networks (red, blue, and green large circles). Depending on the repertoire of splicing factors in each neuronal cell (small circles at bottom), combinatorial control of the exon networks creates diverse isoform repertoires.

Moreover, in some cases, studying individual targeted alternative splicing events may also reveal neuronal phenotypes of interest mediated by alternative splicing, exemplified by our observations that *unc-64* isoforms have nonoverlapping functions (Figure 6E).

Such discovery-driven genetic analyses of exon networks have remained challenging to conduct in vertebrate models in vivo. For example, this study reveals a previously unknown role for the fatty acid CoA synthetase ACS-13 in maintaining proper aldicarb sensitivity. ACSL5, the human homolog of ACS-13, plays a role in fatty acid metabolism and lipid biosynthesis (Yamashita et al., 2000). While it is not immediately clear what mechanistic role *acs-13* may be playing in *C. elegans* neuronal function, a link between the relative concentrations of long-chain fatty acids in neurons and effects on cholinergic synaptic transmission has been described in *C. elegans* (Lesa et al., 2003). It will be interesting to determine whether *acs-13* isoforms also play a mechanistic role connecting lipid metabolism and synaptic transmission.

A Role for Combinatorial Control of Alternative Exons in Generating Neuronal Diversity

Our genetic screen has revealed how alternative splicing can be controlled in a neuron-specific manner through the overlapping expression of two splicing factors. Both UNC-75 and EXC-7 have conserved orthologs in humans (the CELF and Hu family of proteins, respectively), which also play a role in alternative splicing, are expressed in the nervous system, and have been implicated in neuronal disorders (Darnell, 2013; Dasgupta and Ladd, 2012). CELF and Hu family members have recently been shown to act together in controlling alternative splicing of exon 23a of the neuronal NF1 gene in mammalian cell culture (Fleming et al., 2012), suggesting that our model of genome-wide combinatorial control by CELF and Hu family members may apply more broadly to the mammalian nervous system as well.

Data from our mRNA-seq experiments indicate that combinatorial control of alternative splicing by UNC-75 and EXC-7 is extensive (Figure 4). We expect that other combinations of splicing factors with overlapping expression patterns will act together to fine-tune the properties of different neuronal classes as well. This mechanism may serve to allow a relatively small number of factors with overlapping expression patterns to combinatorially create a large diversity of alternative splicing patterns within most nervous systems (Figure 7B). Future studies that make use of *C. elegans* hold promise for yielding insights into the mechanisms governing alternative splicing regulation within the nervous system and the identification of functionally important genes and isoforms in distinct neuron classes.

EXPERIMENTAL PROCEDURES

Strain Maintenance and Microscopy

C. elegans were maintained by standard techniques (Brenner, 1974) on nematode growth medium (NGM) agar plates seeded with OP50 *E. coli*. All images of two-color reporter transgene-expressing animals were captured with a Zeiss Axioskop 2 fluorescence compound microscope and processed in ImageJ.

Mutagenesis and Screening

P_0 worms expressing the *unc-16* exon 16 alternative splicing reporter were mutagenized with EMS at 47 mM for 4 hr. Single F_1s were sorted into individual wells of a 96-well plate by a Union Biometrica COPAS worm sorter. After 4–7 days of growth in NGM liquid culture media at room temperature, an aliquot of each well was transferred to an optical imaging 96-well plate (Nunc). The *unc-16* alternative splicing reporter pattern in the pool of F_2–F_3 mutant worms was analyzed fluorescently on a Zeiss Axioskop 2 microscope. Wells containing mutant animals with altered reporter patterns were isolated. To identify causative mutations, we performed whole-genome sequencing using the software MAQgene according to protocols described elsewhere (Bigelow et al., 2009).

mRNA-Seq Analysis to Identify Differential Junction Usage

Total RNA was isolated from synchronized L4 worms using Tri reagent (Sigma Aldrich), and cDNA libraries from Poly A+ enriched RNA were prepared using the TruSeq RNA kit (Illumina) according to the manufacturer's instructions. Deep sequencing was performed on an Illumina HiSeq 2000 according to standard protocols, generating 150 base paired-end reads. Reads were mapped to the *C. elegans* genome (version WS190) using the RNA-Seq Unified Mapper under default settings (Grant et al., 2011). Alternative junctions were identified using a custom-developed pipeline. For more details, see the Supplemental Information.

Phenotypic Analyses

Aldicarb assays were performed as described elsewhere (Loria et al., 2003) on plates of young adult worms at 15°C and 1 mM aldicarb. A total of 20–30 worms were counted in each assay for each strain, and each assay was replicated a total of three times. Worms were considered paralyzed if they did not move in response to a light nose touch. Coordination assays were performed by placing young adult worms in a drop of M9 buffer and, after 1 min of equilibration, by counting the thrashing rate (frequency of number of body bends per minute) of animals recorded under a stereomicroscope. A total of 15–20 worms were analyzed from each strain tested.

Electrophysiology

The dissection of the *C. elegans* was described elsewhere (Richmond and Jorgensen, 1999). The recording solutions were as described in previous studies (Gao and Zhen, 2011). Specifically, the pipette solution contains the following (in millimolars): 115 K-gluconate; 25 KCl; 0.1 $CaCl_2$; 5 $MgCl_2$; 1 BAPTA; 10 HEPES; 5 Na_2ATP; 0.5 Na_2GTP; 0.5 cAMP; 0.5 cGMP (pH 7.2, with KOH); osmolality, ~320 mOsm · kg^{-1}. The bath solution consists of the following (in millimolars): 150 NaCl; 5 KCl; 5 $CaCl_2$; 1 $MgCl_2$; 10 glucose; 5 sucrose; 15 HEPES (pH 7.3, with NaOH); osmolality, ~330 mOsm · kg^{-1}. Under these conditions, the reversal potentials are ~20 mV for acetylcholine receptors (Gao and Zhen, 2011). Light stimulation of *zxIs6* was performed with an LED lamp (KSL-70; RAPP OptoElectronic) at a wavelength of 470 nm (8 mW/mm^2), controlled by the Axon amplifier software. *zxIs6* was cultured in the dark at 22°C on OP50-seeded NGM plates supplemented with all-*trans* retinal as described elsewhere (Gao and Zhen, 2011). All chemicals were from Sigma. Experiments were performed at room temperatures (20°C–22°C).

ACCESSION NUMBERS

All raw reads (in fastq format) have been deposited to the National Center for Biotechnology Information short-read archive under accession number SRX514835.

SUPPLEMENTAL INFORMATION

Supplemental Information includes Supplemental Experimental Procedures, seven figures, four tables, and one movie and can be found with this article online at http://dx.doi.org/10.1016/j.molcel.2014.05.004.

ACKNOWLEDGMENTS

We thank Ben Blencowe, Andrew Murray, Vlad Denic, Bodo Stern, Nicolas Chevrier, Peter Turnbaugh, Lauren O'Connell, Arneet Saltzman, Joe Calarco, and Xico Gracida for critical reading of the manuscript. Some strains were provided by the Caenorhabditis Genome Center, which is funded by the NIH Office of Research Infrastructure Programs (P40 OD010440). Other strains were provided by the National BioResource Project (Tokyo). M.Z. is supported by grants from the Natural Sciences and Engineering Research Council and the Canadian Institutes of Health Research. J.A.C. is supported by an NIH Director's Early Independence Award (DP5OD009153) and by Harvard University.

Received: January 22, 2014
Revised: March 4, 2014
Accepted: April 24, 2014
Published: June 5, 2014

REFERENCES

Aoto, J., Martinelli, D.C., Malenka, R.C., Tabuchi, K., and Südhof, T.C. (2013). Presynaptic neurexin-3 alternative splicing trans-synaptically controls postsynaptic AMPA receptor trafficking. Cell *154*, 75–88.

Barberan-Soler, S., and Zahler, A.M. (2008). Alternative splicing regulation during C. elegans development: splicing factors as regulated targets. PLoS Genetics *4*, e1000001.

Barberan-Soler, S., Medina, P., Estella, J., Williams, J., and Zahler, A.M. (2011). Co-regulation of alternative splicing by diverse splicing factors in Caenorhabditis elegans. Nucleic Acids Res. *39*, 666–674.

Barbosa-Morais, N.L., Irimia, M., Pan, Q., Xiong, H.Y., Gueroussov, S., Lee, L.J., Slobodeniuc, V., Kutter, C., Watt, S., Colak, R., et al. (2012). The evolutionary landscape of alternative splicing in vertebrate species. Science *338*, 1587–1593.

Bigelow, H., Doitsidou, M., Sarin, S., and Hobert, O. (2009). MAQGene: software to facilitate C. elegans mutant genome sequence analysis. Nat. Methods *6*, 549.

Boucard, A.A., Chubykin, A.A., Comoletti, D., Taylor, P., and Südhof, T.C. (2005). A splice code for trans-synaptic cell adhesion mediated by binding of neuroligin 1 to alpha- and beta-neurexins. Neuron *48*, 229–236.

Boutz, P.L., Stoilov, P., Li, Q., Lin, C.H., Chawla, G., Ostrow, K., Shiue, L., Ares, M., Jr., and Black, D.L. (2007). A post-transcriptional regulatory switch in polypyrimidine tract-binding proteins reprograms alternative splicing in developing neurons. Genes Dev. *21*, 1636–1652.

Braunschweig, U., Gueroussov, S., Plocik, A.M., Graveley, B.R., and Blencowe, B.J. (2013). Dynamic integration of splicing within gene regulatory pathways. Cell *152*, 1252–1269.

Brenner, S. (1974). The genetics of Caenorhabditis elegans. Genetics *77*, 71–94.

Calarco, J.A., Superina, S., O'Hanlon, D., Gabut, M., Raj, B., Pan, Q., Skalska, U., Clarke, L., Gelinas, D., van der Kooy, D., et al. (2009). Regulation of vertebrate nervous system alternative splicing and development by an SR-related protein. Cell *138*, 898–910.

Charlet-B., N., Logan, P., Singh, G., and Cooper, T.A. (2002). Dynamic antagonism between ETR-3 and PTB regulates cell type-specific alternative splicing. Mol. Cell *9*, 649–658.

Chih, B., Gollan, L., and Scheiffele, P. (2006). Alternative splicing controls selective trans-synaptic interactions of the neuroligin-neurexin complex. Neuron *51*, 171–178.

Darnell, R.B. (2013). RNA protein interaction in neurons. Annu. Rev. Neurosci. *36*, 243–270.

Dasgupta, T., and Ladd, A.N. (2012). The importance of CELF control: molecular and biological roles of the CUG-BP, Elav-like family of RNA-binding proteins. Wiley Interdiscip. Rev. RNA *3*, 104–121.

Fleming, V.A., Geng, C., Ladd, A.N., and Lou, H. (2012). Alternative splicing of the neurofibromatosis type 1 pre-mRNA is regulated by the muscleblind-like proteins and the CUG-BP and ELAV-like factors. BMC Mol. Biol. *13*, 35.

Fujita, M., Kawano, T., Ohta, A., and Sakamoto, H. (1999). Neuronal expression of a Caenorhabditis elegans elav-like gene and the effect of its ectopic expression. Biochem. Biophys. Res. Commun. *260*, 646–652.

Fujita, M., Hawkinson, D., King, K.V., Hall, D.H., Sakamoto, H., and Buechner, M. (2003). The role of the ELAV homologue EXC-7 in the development of the Caenorhabditis elegans excretory canals. Dev. Biol. *256*, 290–301.

Gao, S., and Zhen, M. (2011). Action potentials drive body wall muscle contractions in Caenorhabditis elegans. Proc. Natl. Acad. Sci. USA *108*, 2557–2562.

Gehman, L.T., Stoilov, P., Maguire, J., Damianov, A., Lin, C.H., Shiue, L., Ares, M., Jr., Mody, I., and Black, D.L. (2011). The splicing regulator Rbfox1 (A2BP1) controls neuronal excitation in the mammalian brain. Nat. Genet. *43*, 706–711.

Gerstein, M.B., Lu, Z.J., Van Nostrand, E.L., Cheng, C., Arshinoff, B.I., Liu, T., Yip, K.Y., Robilotto, R., Rechtsteiner, A., Ikegami, K., et al.; modENCODE Consortium (2010). Integrative analysis of the Caenorhabditis elegans genome by the modENCODE project. Science *330*, 1775–1787.

Golgi, C. (1883). Sulla fina anatomia degli organi centrali del sistema nervoso [On the fine anatomy of the central organs of the nervous system]. Riv. Sper. Freniat. *9*, 1–17.

Goodman, M.B., Lindsay, T.H., Lockery, S.R., and Richmond, J.E. (2012). Electrophysiological methods for Caenorhabditis elegans neurobiology. Methods Cell Biol. *107*, 409–436.

Grant, G.R., Farkas, M.H., Pizarro, A.D., Lahens, N.F., Schug, J., Brunk, B.P., Stoeckert, C.J., Hogenesch, J.B., and Pierce, E.A. (2011). Comparative analysis of RNA-Seq alignment algorithms and the RNA-Seq unified mapper (RUM). Bioinformatics *27*, 2518–2528.

Greig, L.C., Woodworth, M.B., Galazo, M.J., Padmanabhan, H., and Macklis, J.D. (2013). Molecular logic of neocortical projection neuron specification, development and diversity. Nat. Rev. Neurosci. *14*, 755–769.

Hobert, O., Carrera, I., and Stefanakis, N. (2010). The molecular and gene regulatory signature of a neuron. Trends Neurosci. *33*, 435–445.

Jensen, K.B., Dredge, B.K., Stefani, G., Zhong, R., Buckanovich, R.J., Okano, H.J., Yang, Y.Y.L., and Darnell, R.B. (2000). Nova-1 regulates neuron-specific alternative splicing and is essential for neuronal viability. Neuron *25*, 359–371.

Kuroyanagi, H., Kobayashi, T., Mitani, S., and Hagiwara, M. (2006). Transgenic alternative-splicing reporters reveal tissue-specific expression profiles and regulation mechanisms in vivo. Nat. Methods *3*, 909–915.

Kuroyanagi, H., Ohno, G., Sakane, H., Maruoka, H., and Hagiwara, M. (2010). Visualization and genetic analysis of alternative splicing regulation in vivo using fluorescence reporters in transgenic Caenorhabditis elegans. Nat. Protoc. *5*, 1495–1517.

Kuroyanagi, H., Watanabe, Y., and Hagiwara, M. (2013a). CELF family RNA-binding protein UNC-75 regulates two sets of mutually exclusive exons of the unc-32 gene in neuron-specific manners in Caenorhabditis elegans. PLoS Genet. *9*, e1003337.

Kuroyanagi, H., Watanabe, Y., Suzuki, Y., and Hagiwara, M. (2013b). Position-dependent and neuron-specific splicing regulation by the CELF family RNA-binding protein UNC-75 in Caenorhabditis elegans. Nucleic Acids Res. *41*, 4015–4025.

Lesa, G.M., Palfreyman, M., Hall, D.H., Clandinin, M.T., Rudolph, C., Jorgensen, E.M., and Schiavo, G. (2003). Long chain polyunsaturated fatty acids are required for efficient neurotransmission in C. elegans. J. Cell Sci. *116*, 4965–4975.

Liewald, J.F., Brauner, M., Stephens, G.J., Bouhours, M., Schultheis, C., Zhen, M., and Gottschalk, A. (2008). Optogenetic analysis of synaptic function. Nat. Methods *5*, 895–902.

Loria, P.M., Duke, A., Rand, J.B., and Hobert, O. (2003). Two neuronal, nuclear-localized RNA binding proteins involved in synaptic transmission. Curr. Biol. *13*, 1317–1323.

Markovtsov, V., Nikolic, J.M., Goldman, J.A., Turck, C.W., Chou, M.Y., and Black, D.L. (2000). Cooperative assembly of an hnRNP complex induced by a tissue-specific homolog of polypyrimidine tract binding protein. Mol. Cell. Biol. *20*, 7463–7479.

Miura, S.K., Martins, A., Zhang, K.X., Graveley, B.R., and Zipursky, S.L. (2013). Probabilistic splicing of Dscam1 establishes identity at the level of single neurons. Cell *155*, 1166–1177.

Nilsen, T.W., and Graveley, B.R. (2010). Expansion of the eukaryotic proteome by alternative splicing. Nature *463*, 457–463.

Norris, A.D., and Calarco, J.A. (2012). Emerging roles of alternative pre-mRNA splicing regulation in neuronal development and function. Front. Neurosci. *6*, 122.

Ogawa, H., Harada, S., Sassa, T., Yamamoto, H., and Hosono, R. (1998). Functional properties of the unc-64 gene encoding a Caenorhabditis elegans syntaxin. J. Biol. Chem. *273*, 2192–2198.

Ohno, G., Hagiwara, M., and Kuroyanagi, H. (2008). STAR family RNA-binding protein ASD-2 regulates developmental switching of mutually exclusive alternative splicing in vivo. Genes Dev. *22*, 360–374.

Orengo, J.P., Bundman, D., and Cooper, T.A. (2006). A bichromatic fluorescent reporter for cell-based screens of alternative splicing. Nucleic Acids Res. *34*, e148.

Raj, B., O'Hanlon, D., Vessey, J.P., Pan, Q., Ray, D., Buckley, N.J., Miller, F.D., and Blencowe, B.J. (2011). Cross-regulation between an alternative splicing activator and a transcription repressor controls neurogenesis. Mol. Cell *43*, 843–850.

Ramani, A.K., Calarco, J.A., Pan, Q., Mavandadi, S., Wang, Y., Nelson, A.C., Lee, L.J., Morris, Q., Blencowe, B.J., Zhen, M., and Fraser, A.G. (2011). Genome-wide analysis of alternative splicing in Caenorhabditis elegans. Genome Res. *21*, 342–348.

Ramón y Cajal, S. (1890). Investigaciones de Histología Comparada en Los Centros Ópticos de Los Vertebrados [Comparative Histology Research in the Optical Centers of Vertebrates]. (Madrid, Spain: Consejo Superior de Investigaciones Científicas, Instituto Ramón y Cajal).

Ray, D., Kazan, H., Cook, K.B., Weirauch, M.T., Najafabadi, H.S., Li, X., Gueroussov, S., Albu, M., Zheng, H., Yang, A., et al. (2013). A compendium of RNA-binding motifs for decoding gene regulation. Nature *499*, 172–177.

Richmond, J.E., and Jorgensen, E.M. (1999). One GABA and two acetylcholine receptors function at the C. elegans neuromuscular junction. Nat. Neurosci. *2*, 791–797.

Saifee, O., Wei, L., and Nonet, M.L. (1998). The Caenorhabditis elegans unc-64 locus encodes a syntaxin that interacts genetically with synaptobrevin. Mol. Biol. Cell *9*, 1235–1252.

Shalek, A.K., Satija, R., Adiconis, X., Gertner, R.S., Gaublomme, J.T., Raychowdhury, R., Schwartz, S., Yosef, N., Malboeuf, C., Lu, D., et al. (2013). Single-cell transcriptomics reveals bimodality in expression and splicing in immune cells. Nature *498*, 236–240.

Sieburth, D., Ch'ng, Q., Dybbs, M., Tavazoie, M., Kennedy, S., Wang, D., Dupuy, D., Rual, J.F., Hill, D.E., Vidal, M., et al. (2005). Systematic analysis of genes required for synapse structure and function. Nature *436*, 510–517.

Tursun, B., Cochella, L., Carrera, I., and Hobert, O. (2009). A toolkit and robust pipeline for the generation of fosmid-based reporter genes in C. elegans. PLoS ONE *4*, e4625.

Ule, J., Ule, A., Spencer, J., Williams, A., Hu, J.S., Cline, M., Wang, H., Clark, T., Fraser, C., Ruggiu, M., et al. (2005). Nova regulates brain-specific splicing to shape the synapse. Nat. Genet. *37*, 844–852.

Wang, E.T., Cody, N.A., Jog, S., Biancolella, M., Wang, T.T., Treacy, D.J., Luo, S., Schroth, G.P., Housman, D.E., Reddy, S., et al. (2012). Transcriptome-wide

regulation of pre-mRNA splicing and mRNA localization by muscleblind proteins. Cell *150*, 710–724.

Yamashita, Y., Kumabe, T., Cho, Y.Y., Watanabe, M., Kawagishi, J., Yoshimoto, T., Fujino, T., Kang, M.J., and Yamamoto, T.T. (2000). Fatty acid induced glioma cell growth is mediated by the acyl-CoA synthetase 5 gene located on chromosome 10q25.1-q25.2, a region frequently deleted in malignant gliomas. Oncogene *19*, 5919–5925.

Yano, M., Hayakawa-Yano, Y., Mele, A., and Darnell, R.B. (2010). Nova2 regulates neuronal migration through an RNA switch in disabled-1 signaling. Neuron *66*, 848–858.

Zahler, A.M. (2005). Alternative splicing in C. elegans. WormBook, 1–13.

Zhang, C., Zhang, Z., Castle, J., Sun, S., Johnson, J., Krainer, A.R., and Zhang, M.Q. (2008). Defining the regulatory network of the tissue-specific splicing factors Fox-1 and Fox-2. Genes Dev. *22*, 2550–2563.

Zheng, S., and Black, D.L. (2013). Alternative pre-mRNA splicing in neurons: growing up and extending its reach. Trends Genet. *29*, 442–448.

Zheng, S., Damoiseaux, R., Chen, L., and Black, D.L. (2013). A broadly applicable high-throughput screening strategy identifies new regulators of Dlg4 (Psd-95) alternative splicing. Genome Res. *23*, 998–1007.